Received: 21 November 2016 | Revised: 8 March 2017 | Accepted: 16 March 2017

DOI: 10.1002/humu.23218

RESEARCH ARTICLE

WILEY HGVS HUMAN GENOME VARIATION SOCIETY

Purinergic receptors *P2RX4* and *P2RX7* in familial multiple sclerosis

A Dessa Sadovnick[1,2]* | Ben J Gu[3]* | Anthony L Traboulsee[2]* | Cecily Q Bernales[1] | Mary Encarnacion[1] | Irene M Yee[1] | Maria G Criscuoli[1] | Xin Huang[3] | Amber Ou[3] | Carol J Milligan[3] | Steven Petrou[3] | James S Wiley[3]† | Carles Vilariño-Güell[1]†

[1]Department of Medical Genetics, University of British Columbia, Vancouver, Canada

[2]Division of Neurology, Faculty of Medicine, University of British Columbia, Vancouver, Canada

[3]Florey Institute of Neuroscience and Mental Health, University of Melbourne, Parkville, Victoria, Australia

Correspondence
Carles Vilariño-Güell, 5639-2215 Wesbrook Mall, University of British Columbia, Vancouver, V6T 1Z3, British Columbia, Canada.
Email: carles@can.ubc.ca
Communicated by Christine Van Broeckhoven

*A Dessa Sadovnick, Ben J Gu, and Anthony L Traboulsee are co-first authors.

†James S Wiley and Carles Vilariño-Güell are co-senior authors.

Contract grant sponsors: Canada Research Chair Program (950-228408); Canada Excellence Research Chair Program (214444); Canadian Institutes of Health Research (MOP-137051); Vancouver Coastal Health Research Institute; Milan & Maureen Ilich Foundation (11-32095000); Vancouver Foundation (ADV14-1597); ARC Future Fellowship (FT120100581); NHMRC Project Grant (1048082, 1061419); Victorian Government's Operational Infrastructure Support Grant

Abstract

Genetic variants in the purinergic receptors *P2RX4* and *P2RX7* have been shown to affect susceptibility to multiple sclerosis (MS). In this study, we set out to evaluate whether rare coding variants of major effect could also be identified in these purinergic receptors. Sequencing analysis of *P2RX4* and *P2RX7* in 193 MS patients and 100 controls led to the identification of a rare three variant haplotype (*P2RX7* rs140915863:C>T [p.T205M], *P2RX7* rs201921967:A>G [p.N361S], and *P2RX4* rs765866317:G>A [p.G135S]) segregating with disease in a multi-incident family with six family members diagnosed with MS (logarithm of odds = 3.07). Functional analysis of this haplotype in HEK293 cells revealed impaired P2X7 surface expression ($P < 0.01$), resulting in over 95% inhibition of adenosine triphosphate (ATP)-induced pore function ($P < 0.001$) and a marked reduction in phagocytic ability ($P < 0.05$). In addition, transfected cells showed 40% increased peak ATP-induced inward current ($P < 0.01$), and a greater Ca^{2+} response to the P2X4 135S variant compared with wild type ($P < 0.0001$). Our study nominates rare genetic variants in *P2RX4* and *P2RX7* as major genetic contributors to disease, further supporting a role for these purinergic receptors in MS and the disruption of transmembrane cation channels leading to impairment of phagocytosis as the pathological mechanisms of disease.

KEYWORDS

familial, Mendelian, multiple sclerosis, mutation, P2RX4, P2RX7, P2X4, P2X7, variant

1 | INTRODUCTION

Multiple sclerosis (MS) is a chronic inflammatory disease of the central nervous system (CNS) characterized by myelin loss, axonal pathology, and progressive neurological dysfunction. The etiology of MS is complex with both genetic and environmental factors implicated in disease susceptibility, with the human leucocyte antigen-DRB1 region providing the highest known attributable risk (Traboulsee et al., 2014). Recently, functional variants in genes for the purinergic receptors *P2RX7* (MIM# 602566) and *P2RX4* (MIM# 600846) have been shown to modulate MS susceptibility (Gu et al., 2015). *P2RX7* variants resulting in loss-of-function were found to be protective against MS, particularly rs28360457:G>A (p.R307Q), which has a dominant negative effect on risk of MS, whereas a *P2RX7* rs1718119:G>A (p.A348T) gain-of-function variant increased the risk of disease. In addition, a rare *P2RX4* rs28360472:A>G (p.Y315C) loss-of-function mutation showed a trend toward association, suggesting it increases the risk of MS (Gu et al., 2015; Stokes et al., 2011; Wiley et al., 2011).

The purinergic receptors P2X4 and P2X7 are nonselective transmembrane cation channels with critical roles in immunity and inflammation (Bours, Swennen, Di Virgilio, Cronstein, & Dagnelie, 2006; Burnstock, 2016; Khakh & North, 2006). Activation of P2X7 by extracellular adenosine triphosphate (ATP) leads to pore formation in cells of monocyte-macrophage lineage and triggers a proinflammatory

response, which includes activation of the NALP3 inflammasome, proliferation of B and T cells, and cytokine release (Feske, Skolnik, & Prakriya, 2012; Junger, 2011). However, in the absence of ATP, the P2X7 receptor has an alternative function in the recognition and regulation of apoptotic cell removal that has an important role in early human neurogenesis (Gu, Saunders, Petrou, & Wiley, 2011; Lovelace et al., 2015). Interestingly, postmortem studies have shown a greater density of P2X7 receptors in microglia cells from MS patients compared with controls (Yiangou et al., 2006), further supporting a role for P2X receptors in the mechanism of disease. Given the role of purinergic receptors in the innate and adaptive immune response, and the genetic and biological associations described in MS patients, we studied genetic variants in the *P2RX7-P2RX4* locus by mining exome sequencing data from MS patients and healthy controls. A unique *P2RX7-P2RX4* haplotype, which impairs the phagocytic function of the P2X7 receptor, was found to cosegregate with disease in one family with multiple affected members. While the P2X7 receptor is only one of the many scavenger receptors in the CNS, our data show for the first time that an inherited defect in a scavenger receptor contributes to the pathogenesis of MS.

2 | MATERIAL AND METHODS

2.1 | Participants

A Caucasian case-control series consisting of 2,211 MS patients and 880 unrelated healthy control subjects from Canada were included in this study. Patients were diagnosed with MS according to Poser criteria prior to 2001 (Poser et al., 1983), or McDonald criteria thereafter (McDonald et al., 2001; Polman et al., 2005). The mean age at blood collection was 46.7 ± 11.8 years (SD) for MS patients and 67.2 ± 9.8 years (SD) for controls, with a male to female ratio of 1:2.75 and 1:0.96, respectively. The mean age at MS onset was 31.0 ± 9.7 years (SD), with a median Expanded Disability Status Scale score of 3.5 and an average of 4.05 ± 2.59 (SD). Exome sequencing data from 193 unrelated MS patients (51 male and 141 female) and 100 healthy controls (26 male and 74 female) were available for analysis. All samples were collected through the longitudinal Canadian Collaborative Project on the Genetic Susceptibility to Multiple Sclerosis (Sadovnick, Risch, & Ebers, 1998; Traboulsee et al., 2014). The ethical review board at the University of British Columbia approved the study, and all participants provided informed consent.

2.2 | Exome sequencing

Exonic regions were enriched using an Ion AmpliSeq exome kit (57.7 Mb) and sequenced in an Ion Proton sequencer (Life Technologies, Carlsbad, CA) with a minimum average coverage of 70 reads per base and an average read length of 150 bases. The Ion Torrent Server was used to map reads to NCBI Build 37.1 reference genome and identify variants differing from the reference (Forwell et al., 2016). Annotation of variants was performed with ANNOVAR (Wang, Li, & Hakonarson, 2010), and damage prediction on protein function was assessed using Combined Annotation Dependent Depletion (CADD v1.3) (http://cadd.gs.washington.edu) (Kircher et al., 2014). All variants of interest were confirmed by Sanger sequencing as previously described (Trinh et al., 2013).

2.3 | Linkage analysis

Two-point logarithm of odds (LOD) score was obtained with MLINK assuming a dominant model, with a fully penetrant mutation and without phenocopies, as previously described (Chartier-Harlin et al., 2011; Ott, 1989; Wang et al., 2016). The deleterious allele was defined with a 0.0001 frequency, and the marker-allele frequencies were determined empirically from genotyped individuals within the family.

2.4 | Ethidium uptake

ATP-induced ethidium uptake assays were performed on HEK293 cells transfected with 4 μg P2X7-AcGFP plasmid DNA and/or 0.5 μg P2X4-AcGFP plasmid DNA. The pAcGFP-N1 vector (0.2 μg) was used as the mock-transfected control, using linear polyethylenimine as described previously (Gu et al., 2015). Cell suspensions (1.0 ml) in HEPES-buffered KCl medium (150 mM KCl, 10 mM HEPES, pH 7.5, plus 5 mM D-glucose, 0.1% BSA) were added to the cuvette of a Time Zero module and gently stirred with temperature maintained at 37°C. Ethidium (25 μM) was added, followed by the addition of 1.0 mM ATP 40 sec later. Cells were analyzed at 1,000 events/sec on a FACSCalibur flow cytometer and were gated by forward and side scatter. The linear mean channel of fluorescencey intensity (0–255 channel) of $AcGFP^+$ cells over successive 5 sec intervals was analyzed by WinMDI software, and was plotted against time as previously described (Gu, Rathsam, Stokes, McGeachie, & Wiley, 2009). Paired Student's *t*-test of the area under ATP-induced ethidium uptake curves were used to calculate statistical differences between P2X7 mutant constructs and wild type P2X7 or P2X4-P2X7 constructs and wild type P2X4-P2X7.

2.5 | P2X7 surface expression

Surface expression of the P2X7 receptor was measured by equilibrium binding of the Alexa 647-conjugated P2X7 monoclonal antibody to transfected HEK293 cells. Transfected cells were incubated with Alexa 647 monoclonal anti-P2X7 antibody (Clone L4, 6 μg/ml) for 20 min at 4°C, washed once and analyzed by two-color flow cytometry with gating on AcGFP+ cells. Statistical differences between mutant constructs and equivalent wild type transfections were assessed using Student's *t*-test.

2.6 | Phagocytosis of yellow-orange beads by transfected HEK293 cells

Transfected HEK293 cells (~2×10^6/ml) were resuspended in HEPES-buffered NaCl medium (145 mM NaCl, 5 mM KCl, 10 mM HEPES, pH 7.5, plus 5 mM D-glucose, 0.1% BSA, 0.1 mM $CaCl_2$). For phagocytosis

assay, 5 μl 1.0 μm carboxylated yellow-orange (YO) beads (Polyscience, Taipei, Taiwan) were added at zero time. The linear mean channel of fluorescence intensity for gated AcGFP$^+$ HEK293 cells over successive 10 sec intervals was analyzed by WinMDI software and plotted against time, as described previously (Gu et al., 2014). Paired student's *t*-test was used to assess differences between mutant and wild type constructs.

2.7 | Ca^{2+} influx assay

HEK293 cells were transfected with pAcGFP-N1 (mock), P2X4-WT-AcGFP, and P2X4-135S-AcGFP constructs. Cells (2×10^6) were incubated in Ca^{2+}-free Na medium (145 mM NaCl, 5 mM KCl, 10 mM HEPES, pH 7.5, supplemented with 0.1% BSA and 5 mM glucose) with Fura-Red acetoxymethyl ester (1 μg/ml) for 30 min at 37°C. After one wash, cells were kept at 37°C for another 30 min followed by a second wash. Cells were resuspended in 1 ml Na medium and were analyzed by a FACSCalibur flow cytometer with a Time Zero module (Cytek Biosciences, Fremont, CA). $CaCl_2$ (3 mM) was added and the FL3 voltage is adjusted to give a linear mean channel fluorescence intensity of ~700 for the gated AcGFP$^+$ population. ATPγS (100 μM) was added 40 sec later. The mean fluorescence intensity of Fura Red was recorded in every 2 sec and was plotted against time. The data from each run (about 250 sec) was saved into a listmode file and were analyzed with WinMDI software (The Scripps Research Institute, CA). The area above Ca^{2+} influx curve 60 sec after the addition of agonist was calculated as the arbitrary units for quantitation.

2.8 | In vitro electrophysiology

HEK293 cells were transfected with pAcGFP-N1 (mock), P2X4-WT-AcGFP, and P2X4-135S-AcGFP constructs. Forty-eight hours post-transfection, cells were detached using 0.5 ml Accutase® Cell Detachment Solution (Innovative Cell Technologies Inc., San Diego, CA) and resuspended at a density of 1×10^6 to 5×10^7 per milliliter in 50% serum-free media and 50% external recording solution (v/v). The external recording solution comprised (mmol/L): 145 NaCl, 5 KCl, 1 $MgCl_2$, 2 $CaCl_2$, 13 D-glucose, 10 HEPES (pH 7.4 with NaOH; ~298 mOsm). The internal recording solution comprised (mmol/L): 85 NaCl, 60 NaF, 10 EGTA, 10 HEPES (pH 7.2 with NaOH; ~285 mOsm). Solutions were filtered using a 0.2-μm membrane filter (Minisart; Sartorius Stedim Biotech, Goettingen, Germany). Cells were kept in suspension by gentle automatic pipetting. Currents generated by P2X4 receptors were recorded using the Patchliner® (Nanion Technologies, Munich, Germany) in the whole-cell configuration. Medium single-hole planar NPC-16 chips with an average resistance of ~2.5 MΩ were used. Pipette and whole-cell capacitance were fully compensated. Recordings were acquired at 1 kHz with the low-pass filter set to 0.33 kHz in PATCHMASTER (HEKA Instruments Inc., NY) and were performed at room temperature. P2X4 receptor-dependent currents were induced by application of 100 μM ATP. Cells were held at −50 mV. Offline analysis was performed using MATLAB R2015a (The Math Works Inc., Natick, MA) and GraphPad Prism 6 (Molecular Devices, Sunnyvale, CA). Data are shown as means ± standard error of the mean (SEM). Statistical analysis was performed using Student's *t*-test. Statistical differences were considered significant when $P < 0.05$.

3 | RESULTS

3.1 | Genetic analysis of P2RX7 and P2RX4 in MS patients

The human *P2RX7* and *P2RX4* genes are located 23 kb apart on chromosome 12q24.31. *P2RX7* (NM_002562.5) contains 13 exons that encode P2X7, a protein 595 amino acids in length. *P2RX4* (NM_002560.2) has 12 exons and encodes a 388 amino acid protein, P2X4. Exome sequencing in 193 MS probands and 100 controls resulted in an average sequencing depth of 156.9 ± 90.2 reads (SD) for *P2RX7* and 133.2 ± 86.7 (SD) for *P2RX4*. All coding exons were comprehensively sequenced with the exception of *P2RX7* exon 12 and *P2RX4* exon 1, which presented an average depth of 9.4 ± 5.2 (SD) and 6.0 ± 7.8 (SD), respectively. Exome analysis identified 23 missense substitutions in *P2RX7* and four in *P2RX4* (Table 1). Of those, 12 were exclusively identified in MS patients and were assessed for segregation with disease in additional family members when available (Supp. Fig. S1). Seven variants were considered not to segregate with disease as they were present in at least two unaffected blood-related family members (excluding obligate carriers), or were not observed in at least two family members diagnosed with MS. All remaining variants (*P2RX7* rs140915863:C>T [p.T205M], rs146725537:T>C [p.Y288H], rs201921967:A>G [p.N361S], rs34219304:G>A [p.V522I], and *P2RX4* rs765866317:G>A [p.G135S]) were genotyped in a case-control series consisting of 2,211 MS patients and 880 healthy controls. P2X7 p.Y288H and p.V522I were identified at similar frequencies in MS patients and controls (Supp. Table S1), thus suggesting they are both rare polymorphisms of no effect toward the pathogenesis or susceptibility to MS. P2X7 p.T205M, p.N361S, and P2X4 p.G135S, which are found on a single haplotype, were not observed in any additional subjects. This *P2RX7-P2RX4* three variant haplotype was identified in five family members diagnosed with MS, one obligate carrier and only one out of seven seemingly healthy blood relatives from a single family (Fig. 1A). One additional family member diagnosed with MS was known to exist (III-8), but was deceased at the time of data collection.

To determine whether any other variant could be ascribed to the high prevalence of disease observed in this family, we performed exome sequencing analysis in all additional family members diagnosed with MS for whom a DNA sample was available (III-3–6; Fig. 1A). The pattern of disease inheritance in this family is suggestive of an autosomal-dominant trait with reduced penetrance; therefore, only rare heterozygote coding substitutions identified in all affected individuals were considered potentially pathogenic; detailed methodology has been previously described (Wang et al., 2016). Exome analysis identified a total of 82,073 variants across all five affected subjects, with 3,548 autosomal heterozygote genotypes being observed in all family members examined. After excluding noncoding and silent substitutions, as well as variants with a reported minor allele

TABLE 1 *P2RX7* and *P2RX4* variants identified in MS patients and healthy controls

Chromosome: position	cDNA change	Amino acid change	dbSNP rs ID	ExAC MAF	Controls MAF	MS MAF
P2RX7						
12:121592689	c.227T>C	p.V76A	rs17525809	0.0597	0.081	0.078
12:121593936	c.349C>T	p.R117W	rs28360445	0.0013	0.005	0.010
12:121598715	c.374G>T	p.R125L	rs201668926	2.47×10^{-5}	0	0.003*
12:121600233	c.443A>G	p.Q148R	rs150235326	2.49×10^{-5}	0	0.003*
12:121600238	c.448G>A	p.G150R	rs28360447	0.0127	0	0.016*
12:121600253	c.463C>T	p.H155Y	rs208294	0.4757	0.409	0.422
12:121603240	c.614C>T	p.T205M	rs140915863	0.0005	0	0.003*
12:121605337	c.791G>A	p.R264H	rs149639375	0.0002	0	0.003*
12:121605355	c.809G>A	p.R270H	rs7958311	0.2448	0.278	0.313
12:121605373	c.827G>A	p.R276H	rs7958316	0.0177	0.010	0.016
12:121605408	c.862T>C	p.Y288H	rs146725537	0.0019	0	0.003*
12:121613229	c.920G>A	p.R307Q	rs28360457	0.0081	0.030	0.021
12:121615103	c.1042G>A	p.A348T	rs1718119	0.3582	0.354	0.298
12:121615131	c.1070C>G	p.T357S	rs2230911	0.1323	0.081	0.078
12:121615143	c.1082A>G	p.N361S	rs201921967	8.24×10^{-6}	0	0.003*
12:121622115	c.1298C>T	p.A433V	rs28360459	0.0109	0.005	0.003
12:121622196	c.1379A>G	p.Q460R	rs2230912	0.1318	0.136	0.132
12:121622304	c.1487A>C	p.E496A	rs3751143	0.1903	0.162	0.189
12:121622380	c.1563C>G	p.H521Q	rs2230913	0.0132	0.005	0.003
12:121622381	c.1564G>A	p.V522I	rs34219304	0.0035	0	0.003*
12:121622421	c.1604C>T	p.A535V	rs201256156	0.0004	0	0.003*
12:121622448	c.1631G>A	p.R544Q	rs34567077	3.04×10^{-5}	0	0.003*
12:121622520	c.1703T>A	p.I568N	rs1653624	0.0149	0.040	0.023
P2RX4						
12:121647974	c.7G>T	p.G3C	rs200492184	0.0089	0.005	0
12:121659945	c.403G>A	p.G135S	rs765866317	3.32×10^{-5}	0	0.003*
12:121666646	c.724A>G	p.S242G	rs25644	0.1566	0.136	0.106
12:121670276	c.944A>G	p.Y315C	rs28360472	0.0091	0	0.018*

Notes: Genomic coordinates are given from NCBI Build 37.1; RNA and protein position are based on GenBank RefSeq NM_002562.5 (*P2RX7*) and NM_002560.2 (*P2RX4*); dbSNP IDs are provided from build 149; minor allele frequencies (MAF) were obtained from The Exome Aggregation Consortium (ExAC) database. Variants assessed for segregation are indicated with an asterisk.

frequency over 1% in proprietary and public databases (Lek, Karczewski, Minikel, & Samocha, 2015), only the three variants on the *P2RX7-P2RX4* haplotype were found to be present in all five family members diagnosed with MS. Parametric linkage analysis resulted in a maximum LOD score of 3.07, confirming the cosegregation of this haplotype with disease, thus indicating the variants in this haplotype as the most likely pathogenic mechanism of disease for this family. In silico analysis of these variants found P2X7 p.T205M to be evolutionarily conserved in mammals (Fig. 1B) and predicted likely damaging to protein function with a phred-scaled CADD score of 25.8, whereas P2X7 p.N361S is neither evolutionarily conserved nor predicted damaging (CADD = 0.003). P2X4 p.G135S is predicted deleterious to protein function (CADD = 28.0) and shows the highest level of conservation among these three mutations, with the glycine residue being observed not only in vertebrates but also in all human paralogs.

3.2 | Clinical phenotype for *P2RX7-P2RX4* patients

The family harboring the *P2RX7-P2RX4* disease haplotype is of mixed European/Acadian ancestry. The mean age at the onset of MS was 31.4 ± 8.9 years (SD) with a range of 22–44 (Fig. 1A). Two family members were deceased by the age of 48 (III-6) and 57 years (III-8), 21 and 35 years after the onset of MS, respectively. Detailed clinical phenotype was available for three family members (III-4, III-6, and III-9), and was consistent with a relapsing-remitting course that became progressive for III-6 and III-9 within 15 and 13 years from onset, respectively. The initial symptoms for III-4 and III-6 were sensory disturbances, whereas III-9 presented slowness of movements at the onset of MS. Two seemingly unaffected mutation carriers were also identified (II-2 and III-13). Biological samples from these two family members were collected at 76 (II-2) and 51 (III-13) years of age, and MS symptoms were not reported at collection, thus indicating that the *P2RX7-P2RX4* three mutation haplotype has reduced penetrance.

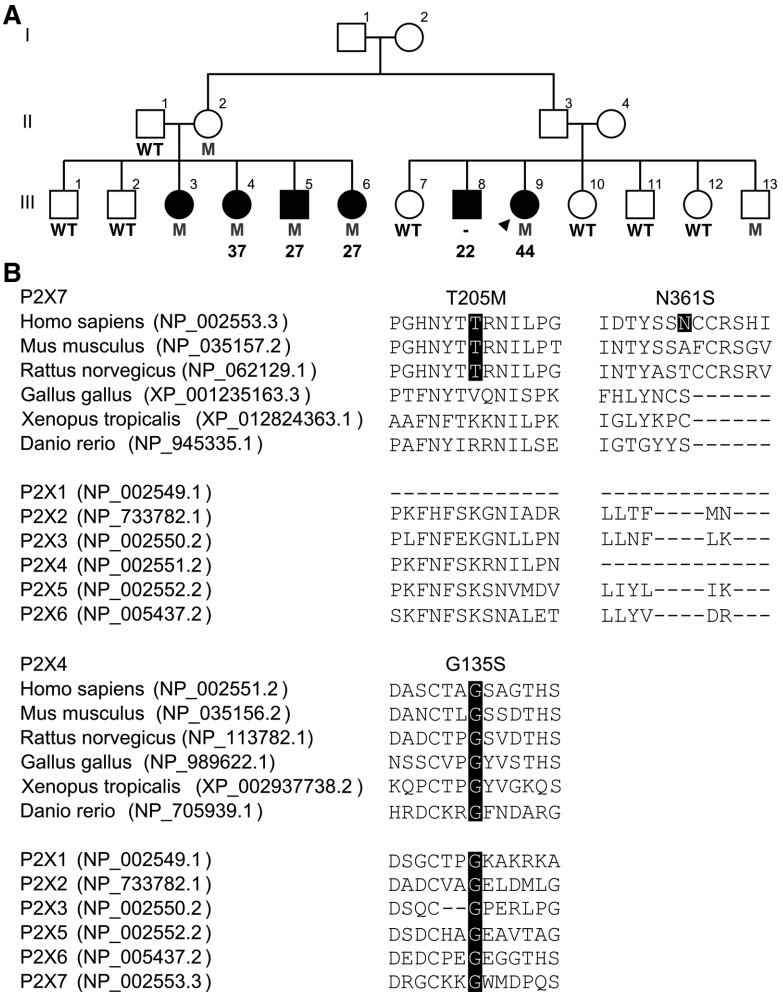

FIGURE 1 Pedigree presenting the P2X7 p.T205M, P2X7 p.N361S, and P2X4 p.G135S haplotype and protein conservation. A: Males are represented by squares and females by circles with the proband indicated win an arrow head. Patients diagnosed with MS have black-filled symbols with corresponding age at onset of disease when available. Heterozygote carriers for all three mutations (M) and wild type (WT) haplotypes are indicated. B: Conservation of P2X7 and P2X4 variants in orthologs and human paralogs are highlighted in black. Protein homologs were aligned via ClustalO, and RefSeq accession numbers are provided

3.3 | A unique *P2RX7-P2RX4* haplotype confers major inhibition on P2X7 pore function

Activation of P2X7 by ATP induces pore formation in cells of monocytic/microglia lineage, which has downstream effects including formation of the NALP3 inflammasone and secretion of proinflammatory cytokines (Mariathasan et al., 2006). We examined P2X7 pore formation by measuring ATP-induced ethidium uptake in HEK293 cells transfected with wild type or mutated P2X7 and/or P2X4 constructs. The P2X7 205M variant conferred greater than 80% inhibition of P2X7-mediated ethidium uptake ($P = 0.0003$), whereas P2X7 361S constructs gave the same ethidium uptake as cells transfected with wild type P2X7 (Fig. 2A). Transfection of HEK293 cells with P2X7 205M plus 361S double-mutant constructs resulted in approximately 70% inhibition of P2X7 pore function compared with wild type ($P = 0.011$). The greatest inhibition of pore function (>95%) was observed when this double P2X7 mutant was cotransfected with P2X4 135S to reproduce the full *P2RX7-P2RX4* haplotype observed in MS patients ($P = 0.008$). Our data show that the P2X7 205M variant is the major contributor to the inhibition of P2X7 pore function, an inhibition that is observed in the absence or presence of variant P2X4 135S. In contrast, P2X7 361S appears to have little or no effect on P2X7 pore function.

3.4 | The P2X7 205M-361S variant fails to express on the surface of transfected HEK293 cells

We measured the surface expression of the P2X7 receptor in transfected HEK293 cells by the binding of Alexa-647-conjugated monoclonal antibody (Clone L4) specific for the extracellular domain of P2X7 (Buell et al., 1998). Identical expression of wild type P2X7 either with or without the 361S mutation was observed in HEK293 cells, and there was a trend to lower values in cells cotransfected with the P2X4 constructs, either wild type or 135S mutant (Fig. 2B). A major reduction in surface expression was found in cells expressing the 205M mutation of P2X7. An identical major reduction in P2X7 expression was observed in cells harboring 205M either with or without the 361S mutation or in P2X7 205M 361S cells cotransfected with P2X4 135S

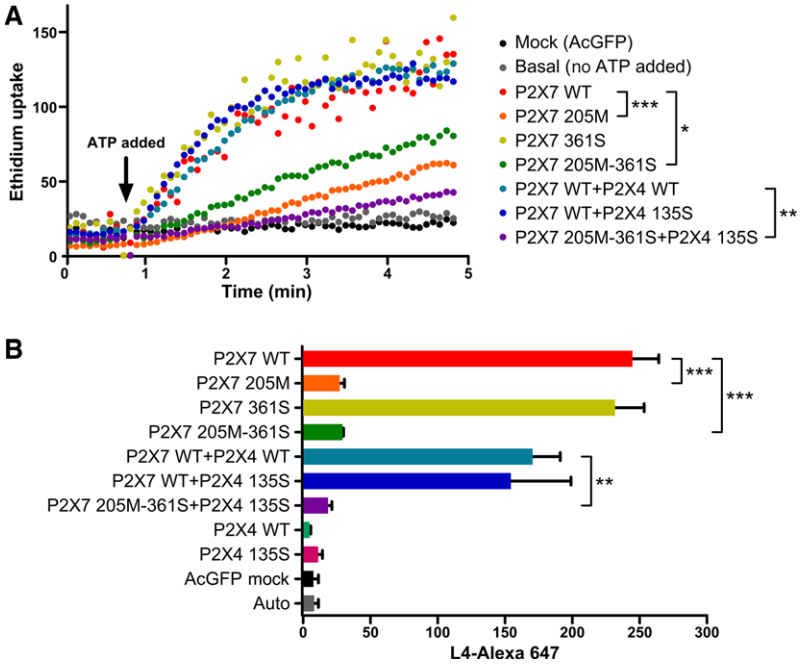

FIGURE 2 P2X7 functional assay. A: ATP-induced ethidium uptake was used to measure P2X7 pore formation in HEK293 cells transfected with various P2X7 and/or P2X4 constructs. The mean fluorescent intensity of ethidium uptake into cells was measured at 5 sec intervals by two-color flow cytometry. B: P2X7 expression on the surface of HEK 293 cells transfected with AcGFP-tagged P2X7 and/or P2X4 constructs. Bars represent mean values and SEM of three replicate experiments. WT, wild type. $^{*}P < 0.05$, $^{**}P < 0.01$; $^{***}P < 0.001$

($P = 0.002$–0.0004). Confocal microscopy confirmed surface expression of P2X7 in wild type and 361S transfected cells, whereas P2X7 constructs containing the 205M variant did not show detectable surface expression (Supp. Fig. S2). This data show that the P2X4 135S and P2X7 361S mutations have no significant effect on P2X7 expression and that the P2X7 205M variant has by far the greatest influence on surface expression of this receptor.

3.5 | Phagocytosis mediated by the P2X7 receptor is abolished by the T205M variant

Phagocytosis mediated by P2X7 requires surface expression of this receptor in a membrane complex that contains nonmuscle myosin IIA and other cytoskeletal proteins (Gu et al., 2009) that allow recognition and engulfment of apoptotic cells or latex beads in the absence of extracellular ATP (Gu et al., 2011; Gu, Saunders, Jursik, & Wiley, 2010). We assayed this scavenger role of P2X7 by measuring the phagocytosis of nonopsonized YO fluorescent beads in HEK293 cells transfected with the same P2X7 and P2X4 constructs previously described. Wild type P2X7 transfected HEK293 cells, as well as P2X7 361S and all P2X4 constructs, showed brisk engulfment of beads at 37°C, whereas cells transfected with any combination of constructs containing P2X7 205M showed significantly impaired bead uptake ($P < 0.05$) (Supp. Figs. S3 and S4).

3.6 | Functional studies on the P2X4 135S variant

P2X4 and P2X7 receptors have been reported to interact on the surface of immune cells eliciting changes in function, but not expression levels of P2X7 (Guo, Masin, Qureshi, & Murrell-Lagnado, 2007). The p.G135S mutation was introduced into a human P2X4 plasmid and expressed in HEK293 cells to assess changes in functional responses. Whole-cell patch clamp recordings showed approximately 40% increased peak ATP-induced inward current for P2X4 135S compared with wild type ($P < 0.01$; Fig. 3A). The functional response of the P2X4 135S variant was also assessed by a second technique in which HEK293 cells transfected with P2X4 wild type or 135S were loaded with the Ca^{2+}-sensitive dye Fura Red. The fluorescence response to activation of P2X4 by its specific ligand, ATPγS (100 μM) was measured by real-time flow cytometry, which again showed a greater Ca^{2+} response to the P2X4 135S variant compared with wild type ($P < 0.0001$; Fig. 3B). These data show that the P2X4 135S variant retains its high permeability to Ca^{2+} ions at wild type or greater levels.

4 | DISCUSSION

In this study, we have identified a *P2RX7-P2RX4* haplotype containing three rare missense mutations segregating with disease in a multiincident family with high incidence of MS (Fig. 1A). The data not only show the existence of genetic variants resulting in familial forms of MS, but also highlight a less recognized function of the P2X7 receptor. Our functional studies revealed that the P2X7 205M, P2X7 361S, and P2X4 135S haplotype expressed in HEK293 cells causes near total loss of ATP-induced ethidium uptake, which is the standard assay for the P2X7 proinflammatory actions of this receptor (Fig. 2A). This result was opposite to that expected for the loss of P2X7 pore function, which generally protects rather than promotes secretion of proinflammatory

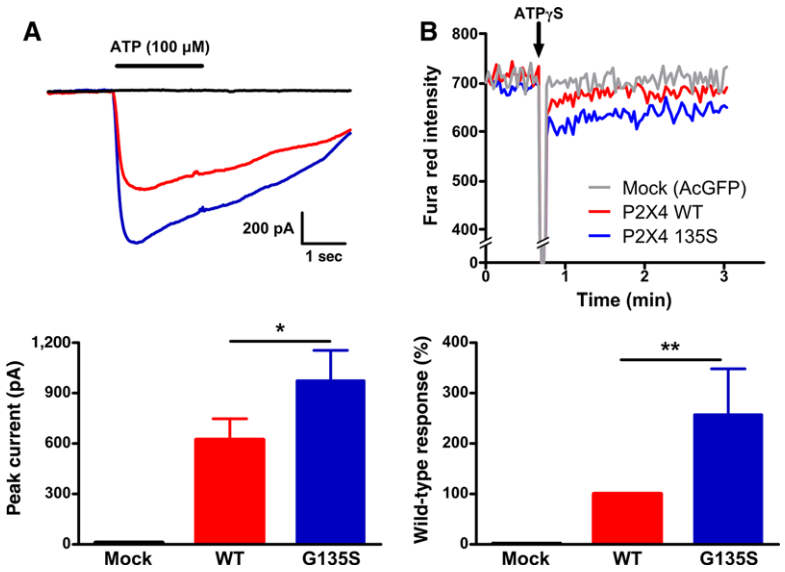

FIGURE 3 P2X4 functional assay using HEK293 cells transfected with AcGFP, wild type P2X4-AcGFP, or P2X4-G135S-AcGFP. A: Whole-cell averaged current traces from mock vector control alone ($n = 6$ cells), P2X4-WT ($n = 6$ cells), and P2X4-G135S ($n = 10$ cells) in response to ATP (100 μM). B: Typical Ca^{2+} influx traces. Ca^{2+} (3 mM) was added 40 sec prior to the addition of 100 μM ATPγS. Normalized Ca^{2+} influx from four separated experiments. $^{*}P < 0.01$; $^{**}P < 0.0001$

cytokines in the CNS (Mariathasan et al., 2006; Qu, Franchi, Nunez, & Dubyak, 2007; Sluyter, Dalitz, & Wiley, 2004), and it is in sharp contrast to our recent genetic study of a P2X7 p.R307Q loss-of-function variant that is associated with a twofold increased protection against the risk of developing MS (Gu et al., 2015). To resolve this paradox, we examined the expression of P2X7 as well as measuring a second function of this receptor, namely, a scavenger function in which P2X7 in the absence of ATP can recognize and regulate the phagocytosis of apoptotic cells (Gu et al., 2010; Gu et al., 2011). Unlike the majority of polymorphic variants such as p.R307Q, which are expressed close to wild type levels on the cell surface, the *P2RX7-P2RX4* haplotype identified in the index family shows near total absence of P2X7 surface expression on HEK293 cells (Fig. 2B). Cells transfected with P2X7 205M constructs failed to bind the monoclonal L4 antibody, which is specific for the extracellular domain of P2X7 (Buell et al., 1998). This result explains the loss of P2X7-mediated ethidium uptake by the mutant haplotype and suggests an impaired trafficking of P2X7 to the cell surface, although accelerated turnover of surface receptors cannot be excluded. Failure of the P2X7 mutant haplotype to express on the cell surface resulted in a major loss of phagocytic ability in HEK293 cells, with the uptake of fluorescent beads being significantly reduced compared with wild type transfected cells. Together, these functional data show the near complete abolition of both pore function and scavenger function is a result of the failure of P2X7 receptors to express on the cell surface. The role of P2X4 p.G135S on P2X7 function appears minor, although there is some evidence of interaction between P2X4 and P2X7 receptors on the surface of immune cells. P2X4 and P2X7 subunits can be coimmunoprecipitated both from transfected and native cells, whereas protein–protein interactions between P2X4 and the carboxyl tail of P2X7 have been shown in FRET experiments (Guo et al., 2007; Perez-Flores et al., 2015). Our data are in line with a previous study (Guo et al., 2007) and show that cotransfection with P2X4 135S and P2X7 205M constructs gave even greater inhibition of pore function compared with P2X7 205M alone. However, this functional interaction of mutant P2X4 and P2X7 did not significantly further reduce the surface expression of P2X7 receptors.

Functional analysis of P2X4 showed that the 135S mutation identified in MS patients resulted in increased ATP-induced inward currents. Although the P2X4 contribution to inflammation appears minor in comparison to P2X7 (Burnstock, 2016; de Rivero Vaccari, Dietrich, & Keane, 2014), disruption of the P2X7-P2X4 interaction has been shown to hinder the physiological response to ATP in immune cells (Perez-Flores et al., 2015), and appears to potentially exacerbate the P2X7 phenotype (Fig. 2A). Further studies are necessary to fully characterize the role and interaction of P2X7 and P2X4 mutations in the onset of MS. However, our study is the first to show impaired phagocytosis as a mechanism of disease for MS, and suggest impaired function of scavenger receptors as one of the critical component in MS pathophysiology.

The pathogenicity of the *P2RX7-P2RX4* haplotype identified in a multi-incident family (Fig. 1A) is supported by a significant cosegregation with MS (LOD = 3.07), disrupted biological functions (Figs. 2 and 3), and previously reported associations between common variants and MS risk (Gu et al., 2015). Functional analysis indicates that P2X7 p.N361S is unlikely to be pathogenic; however, genotyping in additional multi-incident families is necessary to elucidate whether the disease haplotype, P2X7 p.T205M or p.P2X4 p.G135S, is the major genetic contributor to the high prevalence of MS observed in this family. It should also be noted that the identification of two unaffected mutation carriers suggests that additional genetic or environmental factors may be required in addition to this highly susceptible genetic background to trigger the onset of disease.

In summary, our data show that the *P2RX7-P2RX4* three mutation haplotype identified in a multi-incident MS family greatly impairs the

expression of P2X7 on the cell surface, resulting in almost complete abolition of the scavenger function of this archaic purinergic receptor. This is in sharp contrast to previously characterized polymorphisms in these genes, and suggests the disruption of transmembrane cation channels and the impairment of phagocytosis by *P2RX7* and *P2RX4* mutations as a major contributor to the onset of MS.

ACKNOWLEDGMENTS

We are grateful to all individuals who generously participated in this study. We thank Kevin Atkins for data collection and extraction.

REFERENCES

Bours, M. J., Swennen, E. L., Di Virgilio, F., Cronstein, B. N., & Dagnelie, P. C. (2006). Adenosine 5'-triphosphate and adenosine as endogenous signaling molecules in immunity and inflammation. *Pharmacology and Therapeutics*, *112*, 358–404.

Buell, G., Chessell, I. P., Michel, A. D., Collo, G., Salazzo, M., Herren, S., … Humphrey, P. P. (1998). Blockade of human P2X7 receptor function with a monoclonal antibody. *Blood*, *92*, 3521–3528.

Burnstock, G. (2016). P2X ion channel receptors and inflammation. *Purinergic Signalling*, *12*, 59–67.

Chartier-Harlin, M. C., Dachsel, J. C., Vilarino-Guell, C., Lincoln, S. J., Lepretre, F., & Hulihan, M. M., … Farrer M. J. (2011). Translation initiator EIF4G1 mutations in familial Parkinson disease. *The American Journal of Human Genetics*, *89*, 398–406.

de Rivero Vaccari, J. P., Dietrich, W. D., & Keane, R. W. (2014). Activation and regulation of cellular inflammasomes: Gaps in our knowledge for central nervous system injury. *Journal of Cerebral Blood Flow & Metabolism*, *34*, 369–375.

Exome Aggregation Consortium, Lek, M., Karczewski, K., Minikel, E., & Samocha, K. (2015). Analysis of protein-coding genetic variation in 60,706 humans. *Nature*, *536*, 285–291.

Feske, S., Skolnik, E. Y., & Prakriya, M. (2012). Ion channels and transporters in lymphocyte function and immunity. *Nature Reviews Immunology*, *12*, 532–547.

Forwell, A. L., Bernales, C. Q., Ross, J. P., Yee, I. M., Encarnacion, M., Lee, J. D., … Vilarino-Guell, C. (2016). Analysis of CH25H in multiple sclerosis and neuromyelitis optica. *Journal of Neuroimmunology*, *291*, 70–72.

Gu, B. J., Field, J., Dutertre, S., Ou, A., Kilpatrick, T. J., & Lechner-Scott, J., … Wiley J. S. (2015). A rare P2X7 variant Arg307Gln with absent pore formation function protects against neuroinflammation in multiple sclerosis. *Human Molecular Genetics*, *24*, 5644–5654.

Gu, B. J., Rathsam, C., Stokes, L., McGeachie, A. B., & Wiley, J. S. (2009). Extracellular ATP dissociates nonmuscle myosin from P2X7 complex: This dissociation regulates P2X7 pore formation. *American Journal of Physiology Cell Physiology*, *297*, C430–C439.

Gu, B. J., Saunders, B. M., Jursik, C., & Wiley, J. S. (2010). The P2X7-nonmuscle myosin membrane complex regulates phagocytosis of non-opsonized particles and bacteria by a pathway attenuated by extracellular ATP. *Blood*, *115*, 1621–1631.

Gu, B. J., Saunders, B. M., Petrou, S., & Wiley, J. S. (2011). P2X(7) is a scavenger receptor for apoptotic cells in the absence of its ligand, extracellular ATP. *The Journal of Immunology*, *187*, 2365–2375.

Gu, B. J., Sun, C., Fuller, S., Skarratt, K. K., Petrou, S., & Wiley, J. S. (2014). A quantitative method for measuring innate phagocytosis by human monocytes using real-time flow cytometry. *Cytometry Part A*, *85*, 313–321.

Guo, C., Masin, M., Qureshi, O. S., & Murrell-Lagnado, R. D. (2007). Evidence for functional P2X4/P2X7 heteromeric receptors. *Molecular Pharmacology*, *72*, 1447–1456.

Junger, W. G. (2011). Immune cell regulation by autocrine purinergic signalling. *Nature Reviews Immunology*, *11*, 201–212.

Khakh, B. S., & North, R. A. (2006). P2X receptors as cell-surface ATP sensors in health and disease. *Nature*, *442*, 527–532.

Kircher, M., Witten, D. M., Jain, P., O'Roak, B. J., Cooper, G. M., & Shendure, J. (2014). A general framework for estimating the relative pathogenicity of human genetic variants. *Nature Genetics*, *46*, 310–315.

Lovelace, M. D., Gu, B. J., Eamegdool, S. S., Weible, M. W., Wiley, J. S., Allen, D. G., & Chan-Ling, T. (2015). P2X7 receptors mediate innate phagocytosis by human neural precursor cells and neuroblasts. *Stem Cells*, *33*, 526–541.

Mariathasan, S., Weiss, D. S., Newton, K., McBride, J., O'Rourke, K., Roose-Girma, M., … Dixit, V. M. (2006). Cryopyrin activates the inflammasome in response to toxins and ATP. *Nature*, *440*, 228–232.

McDonald, W. I., Compston, A., Edan, G., Goodkin, D., Hartung, H. P., Lublin, F. D., … Wolinsky, J. S. (2001). Recommended diagnostic criteria for multiple sclerosis: Guidelines from the International Panel on the diagnosis of multiple sclerosis. *Annals of Neurology*, *50*, 121–127.

Ott, J. (1989). Computer-simulation methods in human linkage analysis. *Proceedings of the National Academy of Sciences of the United States of America*, *86*, 4175–4178.

Perez-Flores, G., Levesque, S. A., Pacheco, J., Vaca, L., Lacroix, S., Perez-Cornejo, P., & Arreola, J. (2015). The P2X7/P2X4 interaction shapes the purinergic response in murine macrophages. *Biochemical and Biophysical Research Communications*, *467*, 484–490.

Polman, C. H., Reingold, S. C., Edan, G., Filippi, M., Hartung, H. P., Kappos, L., … Wolinsky, J. S. (2005). Diagnostic criteria for multiple sclerosis: 2005 revisions to the "McDonald Criteria". *Annals of Neurology*, *58*, 840–846.

Poser, C. M., Paty, D. W., Scheinberg, L., McDonald, W. I., Davis, F. A., Ebers, G. C., … Tourtellotte, W. W. (1983). New diagnostic criteria for multiple sclerosis: Guidelines for research protocols. *Annals of Neurology*, *13*, 227–231.

Qu, Y., Franchi, L., Nunez, G., & Dubyak, G. R. (2007). Nonclassical IL-1 beta secretion stimulated by P2X7 receptors is dependent on inflammasome activation and correlated with exosome release in murine macrophages. *Journal of Immunology*, *179*, 1913–1925.

Sadovnick, A. D., Risch, N. J., & Ebers, G. C. (1998). Canadian collaborative project on genetic susceptibility to MS, phase 2: Rationale and method. Canadian collaborative study group. *Canadian Journal of Neurological Sciences*, *25*, 216–221.

Sluyter, R., Dalitz, J. G., & Wiley, J. S. (2004). P2X7 receptor polymorphism impairs extracellular adenosine 5'-triphosphate-induced interleukin-18 release from human monocytes. *Genes & Immunity*, *5*, 588–591.

Stokes, L., Scurrah, K., Ellis, J. A., Cromer, B. A., Skarratt, K. K., Gu, B. J., … Wiley, J. S. (2011). A loss-of-function polymorphism in the human P2X4 receptor is associated with increased pulse pressure. *Hypertension*, *58*, 1086–1092.

Traboulsee, A. L., Bernales, C. Q., Ross, J. P., Lee, J. D., Sadovnick, A. D., & Vilarino-Guell, C. (2014). Genetic variants in IL2RA and IL7R affect multiple sclerosis disease risk and progression. *Neurogenetics*, *15*, 165–169.

Trinh, J., Vilarino-Guell, C., Donald, A., Shah, B., Yu, I., Szu-Tu, C., … Farrer, M. J. (2013). STX6 rs1411478 is not associated with increased risk of Parkinson's disease. *Parkinsonism & Related Disorders*, *19*, 563–565.

Wang, K., Li, M., & Hakonarson, H. (2010). ANNOVAR: Functional annotation of genetic variants from high-throughput sequencing data. *Nucleic Acids Research*, *38*, e164.

Wang, Z., Sadovnick, A. D., Traboulsee, A. L., Ross, J. P., Bernales, C. Q., Encarnacion, M., … Vilariño-Güell, C. (2016). Nuclear receptor NR1H3 in familial multiple sclerosis. *Neuron*, *90*, 948–954.

Wiley, J. S., Sluyter, R., Gu, B. J., Stokes, L., & Fuller, S. J. (2011). The human P2X7 receptor and its role in innate immunity. *Tissue Antigens*, *78*, 321–332.

Yiangou, Y., Facer, P., Durrenberger, P., Chessell, I. P., Naylor, A., Bountra, C., … Anand, P. (2006). COX-2, CB2 and P2X7-immunoreactivities are increased in activated microglial cells/macrophages of multiple sclerosis and amyotrophic lateral sclerosis spinal cord. *BMC Neurology*, *6*, 12.

SUPPORTING INFORMATION

Additional Supporting Information may be found online in the supporting information tab for this article.

How to cite this article: Sadovnick AD, Gu BJ, Traboulsee AL, et al. Purinergic receptors *P2RX4* and *P2RX7* in familial multiple sclerosis. *Human Mutation*. 2017;38:736–744. https://doi.org/10.1002/humu.23218